3D SIMULATIONS OF THE IONOSPHERE: SZA VARIABILITY AND THE POST-TERMINATOR IONOSPHERE.

F. González-Galindo, M.A. López-Valverde, G. Gilli, *Instituto de Astrofísica de Andalucía, CSIC, Granada, Spain)***, J.-Y. Chaufray, F. Leblanc,** *Laboratoire Atmospheres, Milieux et Observations Spatiales, Paris, France***, F. Forget,** *Laboratoire de Météorologie Dynamique, CNRS, Paris, France***.**

Introduction

The observations of the ionosphere by the Mars Global Surveyor Radio Science System (MGS RSS), the Mars Express Radio Science Experiment (MaRS) and the Mars Express Advanced Radar for Subsurface and Ionospher Sounding (MARSIS) have allowed a clear characterization of the behavior of the Martian dayside ionosphere. Withers (2009) summarizes the main variabilities affecting this atmospheric region. Focusing on the photochemistry-dominated region (below about 180-200 km of altitude from the surface), the observations clearly show that the peak electron density presents a variation with Solar Zenith Angle (SZA) in good agreement with the expected behavior from a Chapman layer, with significant departures when approaching the terminator. The solar activity, the presence of crustal magnetic fields and the variability of the neutral atmosphere are factors that produce additional ionospheric variability.

The behavior of the ionosphere at twilight close to the terminator (SZA=90-105°) and during nighttime (SZA>105°) is much less known, because the observations are much more scarce. Lillis et al. (2009) summarize the different processes that affect the behavior of the nightside ionosphere. These processes include the neutral atmosphere variability, plasma transport by magnetic fields, precipitating particles and transient events. Gurnett et al. (2008) shows that the electron densities measured by MARSIS for SZA>90° are irregular and well above the predictions of a Chapman's model. Němec et al. (2010) found that the probability of finding peak electron densities higher than MARSIS detection limit decreased with increasing SZA for SZA<125° in regions of weak crustal magnetic field. They concluded that the transport of plasma from the dayside was the dominant source of nightside plasma. Similarly, Withers et al. (2012) show that peak electron densities measured by MaRS decrease with increasing SZA in the range SZA=100-115°, which they also attribute to transport of plasma from the dayside. For higher SZAs MaRS data do not show a clear trend in the peak electron densities, implying that other processes, such as electron precipitation, must be at the origin of the deep nightside ionosphere. Němec et al. (2011) present the first observations of the Martian ionosphere for SZA>125° made by MARSIS. Only about 1% of the MARSIS observations in the deep nightside contain a detectable amount of plasma, indicating that most of the time the plasma densities in the deep nightside are small, below the detection limit of the instrument (around $5{\cdot}10^{-3}$ cm^{-3}). The observations with a detectable ionosphere, corresponding to localized patches of enhanced ionization, are located in regions with an open magnetic field configuration. This is indicative of electron precipitation being the main source of plasma in the deep nightside.

In summary, the nightside ionosphere can be divided in two regions or regimes: the twilight ionosphere, where the peak electron densities decrease with increasing SZA and have typical values below about 10^4 cm^{-3}, and which is attributed to plasma transport; and the deep nightside ionosphere, where usually electron densities are quite low, below the detection limits of current instruments, but where significant local enhancements (densities even $> 5 \cdot 10^4$ cm^{-3} are sometimes produced probably due to electron precipitation.

Our objective is to use a state-of-the-art General Circulation Model, the LMD-MGCM, recently extended to include ionospheric chemistry, to simulate the SZA variability of the Martian ionosphere, paying special attention to the ionospheric behavior after the terminator.

The LMD-MGCM

The LMD-MGCM is a ground-to-exosphere General Circulation Model (GCM) that allows for a self-consistent description of the interactions and couplings between different physical processes and different atmospheric regions. A description of this model can be found in Forget et al. (1999) and González-Galindo et al. (2009). Recently the model has been improved by adding some new physical processes or by refining some of the parameterizations used (Millour et al., 2012; González-Galindo et al., 2013). Here we use the lattest version of the model.

Focusing on the ionosphere, the photochemical model used in the upper atmosphere (González-Galindo et al., 2005) has been extended to include Nitrogen species and ionospheric chemistry (González-Galindo et al., 2013). 92 chemical reactions between 25 chemical species are considered. Photochemical equilibrium is used for the fastest species, and the photodissociation and photoionization rates are self-consistently calculated by the model. A parameterization of the secondary ionization produced by energetic photochemically produced electrons (Nicholson et al., 2009) is included in the model. The

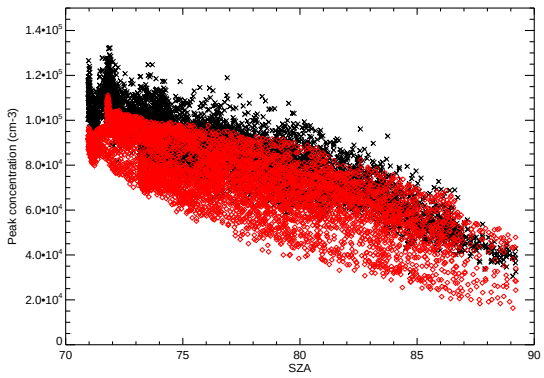

Figure 1: Peak electronic concentration, as a function of SZA, as observed by MGS (black crosses) and as simulated by the LMD-MGCM (red diamonds)

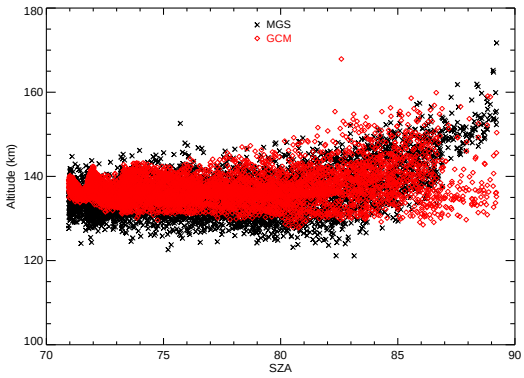

Figure 2: Altitude of the electronic peak, as a function of SZA, as observed by MGS (black crosses) and as simulated by the LMD-MGCM (red diamonds)

ions and electrons are allowed to be transported by the thermospheric winds.

The ionospheric model has some important limitations. The base version does not include any plasma transport process, which limits the validity of the results to the photochemically-dominated region (below about 180 km) and to regions with no strong crustal field. However, the model has been recently extended to include the effect of transport due to pressure gradients (Chaufray et al., 2013), and the effects of including this process on the results will be discussed. Electron precipitation is neither included at this stage.

Selection of results

We first compare the SZA variability of the dayside ionosphere predicted by the model with observations from MGS RSS. For this purpose the model has been run for the period of MGS RSS observations, using the observed day-to-day variability of the solar flux and the observed dust load in the lower atmosphere as inputs. The model results are then interpolated to the exact location (spatial and temporal) of MGS RSS observations, and the peak electron density and the peak altitude predicted by the model are extracted and compared to the observations.

Fig. 1 shows the comparison of the peak electron density predicted by the model with MGS observations, as a function of SZA. The model tends to underestimate the electronic concentration when compared to the observations. The average underestimation is of about 15%. As discussed in González-Galindo et al. (2013) this is mostly due to the poor vertical resolution of the model in the upper atmosphere (about 7km). However, the SZA variability of the data is well reproduced by the model. It is also noteworthy that there are departures of the behavior predicted by a Chapman model. For example, the data show two local maxima in the electronic concentration at about SZA=71° and SZA=73°, and between these values the electronic concentration increases with increasing SZA. This anomalous behavior is linked to the short-term solar variability, and is well reproduced by the model.

The comparison of the altitude of the electronic peak is shown in Fig. 2. The altitude is well reproduced by the model. The average difference of altitude between MGS RSS observations and LMD-MGCM simulations is around 2km, less than half the vertical resolution of the model. Given that the altitude of the peak is mostly influenced by the thermal structure of the atmosphere below the peak, this result indicates that the LMD-MGCM is doing a good job in predicting the temperatures in the lower atmosphere-mesosphere region. Both the data and the model show an increase of the altitude of the peak with increasing SZA, although this behavior is not as clear in the model as in the data. This suggests that the thermal structure around the terminator predicted by the model may not be completely correct.

MGS RSS data are limited to the dayside, so no information can be obtained from them about the nightside ionosphere. MARSIS and MaRS have overcome this limitation and observed in the nightside. The results from the LMD-MGCM have been compared to different analytical fits to MARSIS data in Fig. 15 of González-Galindo et al. (2013). The model reproduces very well the behavior of MARSIS data for all values of SZA until about SZA=105°. For higher values of SZA, the electron density predicted by the model is significantly higher than that in the analytic fits to MARSIS data. However, it has to be taken into account that these fits are only valid for SZA$<100°$ and for higher SZAs they underestimate the measured electron density (Gurnett et al., 2008).

The electron densities measured by MaRS on the

nightside range between about $1.5{\cdot}10^4$ cm^{-3} for SZA$\approx$ 100° to around 3-5 $\cdot 10^3$ cm $^{-3}$ for SZA$\approx$ 115°. The LMD-MGCM results in Fig. 15 of González-Galindo et al. (2013) show average electron densities around $5 \cdot 10^3$ cm^{-3} for SZA$\approx$ 100° and $5-7{\cdot}10^2$ cm^{-3} for SZA$\approx$ 110°, a factor 5 to 10 less than MaRS observations. However, the model predicts a very important variability at high SZAs and MaRS observations fall inside the variability range predicted by the model. It has also to be taken into account that Fig. 15 of González-Galindo et al. (2013) represents the annual mean electron density, that is not necessarily representative of the conditions at the time and location of MaRS observations. In addition, the model used for this comparison does not include the effects of plasma dynamics. When including this process, the electronic concentrations increases in the nightside, at least below 150 km (Chaufray et al., 2013).

Even in the absence of plasma dynamics, the LMD-MGCM predicts the presence of an twilight ionosphere not far from that observed by MARSIS at MaRS for SZA$<$ 120°. The predicted nightside ionosphere is mostly formed by NO^+, that at the altitude of the ionospheric peak has a lifetime long enough to survive during the night. This suggests that photochemistry alone is enough to explain the presence of an ionosphere after the terminator, and the decrease of the electron concentration with increasing SZA, without any need to invoke plasma dynamics processes, at least below about 180 km. However, plasma dynamics can introduce modifications over this photochemically formed ionosphere and popullate it further, as shown by Chaufray et al., (2013). It is also clear that the model can not explain the presence of the areas of enhanced ionization in the deep nightside, where the plasma concentration predicted by the model is of around 10^2 cm^{-3}. Electron precipitation in regions with an open magnetic field configuration remains as its most plausible main formation mechanism.

Acknowledgments

Authors are indebted to the ANR HELIOSARES (ANR-09-BLAN-0223), The French National Program PNST, the French Agency CNES, the CSA and IPSL for their suppor.

References

Chaufray. J.-Y., F. González-Galindo , F. Forget , M.A. López-Valverde , F. Leblanc , R. Modolo , S. Hess , M. Yagi , P.-L. Blelly, and O. Witasse (2013). 3D Martian Ionosphere model : II Effect of transport processes due to pressure gradients. Paper submitted to JGR-Planets.

Forget, F., F. Hourdin, R. Fournier, C. Hourdin, O. Talagrand, M. Collins, S. R. Lewis, P. L. Read, and J.-P. Huot (1999). Improved general circulation models of the Martian atmosphere from the surface to above 80 km, J. Geophys. Res., 104, 24,155-24,176

González-Galindo, F., M. A. López-Valverde, M. Angelats i Coll, and F. Forget (2005). Extension of a martian general circulation model to thermospheric altitudes: UV heating and photochemical models, J. Geophys. Res., 110, E09008.

González-Galindo, F., F. Forget, M. A. López-Valverde, M. Angelats i Coll, and E. Millour (2009). A ground-to-exosphere Martian general circulation model: 1. Seasonal, diurnal, and solar cycle variation of thermospheric temperatures, J. Geophys. Res., 114, E04001.

González-Galindo, F., J.-Y. Chaufray, M. A. López-Valverde, G. Gilli, F. Forget, F. Leblanc, R. Modolo, S. Hess, and M. Yagi (2013). Three-dimensional Martian ionosphere model: I. The photochemical ionosphere below 180 km, J. Geophys. Res. Planets, 118.

Gurnett, D. A., et al. (2008), An overview of radar soundings of the Martian ionosphere from the Mars Express spacecraft, Adv. Space Res., 41, 1335-1346

Lillis, R. J., M. O. Fillingim, L. M. Peticolas, D. A. Brain, R. P. Lin, and S. W. Bougher (2009). Nightside ionosphere of Mars: Modeling the effects of crustal magnetic fields and electron pitch angle distributions on electron impact ionization, J. Geophys. Res., 114, E11009

Němec, F., D. D. Morgan, D. A. Gurnett, and F. Duru (2010). Nightside ionosphere of Mars: Radar soundings by the Mars Express spacecraft, J. Geophys. Res., 115, E12009

Němec, F., D. D. Morgan, D. A. Gurnett, F. Duru, and V. Truhlik (2011). Dayside ionosphere of Mars: Empirical model based on data from the MARSIS instrument, J. Geophys. Res., 116, E07003

Nicholson, W. P., G. Gronoff, J. Lilensten, A. D. Aylward, and C. Simon (2009), A fast computation of the secondary ion production in the ionosphere of Mars, Mon. Not. R. Astron. Soc., 400, 369-382

Withers, P. (2009). A review of observed variability in the dayside ionosphere of Mars, Adv. Space Res., 44, 277-307

Withers, P., M. O. Fillingim, R. J. Lillis, B. HÃ/Usler, D. P. Hinson, G. L. Tyler, M. PÃ/Tzold, K. Peter, S. Tellmann, and O. Witasse (2012). Observations of the nightside ionosphere of Mars by the Mars Express radio science experiment (MaRS), J. Geophys. Res., 117, A12307